Fluorescent Probes

Visualization and Isolation of Langerhans Islets by a Fluorescent Probe PiY**

Nam-Young Kang, Sung-Chan Lee, Sung-Jin Park, Hyung-Ho Ha, Seong-Wook Yun, Elena Kostromina, Natalia Gustavsson, Yusuf Ali, Yogeswari Chandran, Hang-Suk Chun, MyungAe Bae, Jin Hee Ahn, Weiping Han, George K. Radda, and Young-Tae Chang*

Pancreatic Langerhans islets are mainly composed of insulin-secreting beta cells and glucagon-secreting alpha cells, along with other minor cell types, and play a central role in the regulation of blood glucose levels.[1] Because of this, imaging of viable pancreatic islets is an important component in research on diabetes both in clinical and experimental medicine.[2–4] The conventional imaging technique for pancreatic islets is antibody-based immunostaining directly on pancreatic sections,[5] or using transgenic mice with luminescent reporter genes linked to islet-specific promoters.[6] Among small molecule probes, Newport Green[7] and dithiazone (DTZ)[8] have been used for ex vivo fluorescent staining of pancreatic islets, based on their Zn^{2+} ion binding affinity, which are abundant in beta cells in complex with insulin. For in situ application, fluorescently labeled exendin-4 (a GLP-1R binding peptide: M.W. is about 5 kDa) has been recently introduced for the measurement of the mass of pancreatic islet beta cells.[9] However, small molecule probes for selective staining of beta cells in pancreatic islets of live animals have not yet been reported.

We predicted that a diversity-oriented fluorescence library approach (DOFLA), an expedited bioimaging probe discovery method using high throughput synthesis and high contents screening, would be a powerful method to achieve this goal. Using a similar approach, we have previously elucidated probes for pluripotent stem cells (CDy1),[10] muscle cells (CDy2),[11] neuronal stem cells (CDr3),[12] and pancreatic alpha cells (GY = glucagon yellow).[13]

Although the glucagon-targeting probe GY selectively stains alpha cells in isolated cell culture, it did not clearly mark mouse pancreatic islets in tissue, partially owing to the small population of alpha cells (around 15–20% in mouse islets).[14] We expected that a fluorescent probe for pancreatic beta cells (with a larger population of 75–80% in mouse islets)[15] would be more effective for visualizing pancreatic islets. As a first step, we synthesized fluorescent small-molecule libraries composed of 1200 compounds,[16] and screened them against beta TC-6 cells in comparison to alpha TC-1 cells and acinar cells (exocrine cells in the pancreas) as controls.

The three cell types were compared in 384-well plates and incubated with the library compounds (1 μM) at incubation times ranging from one to 48 hours. The fluorescence live-cell images were acquired by an automated imaging microscope system, ImageXpress Micro.

One compound from the BDNCA series (Scheme 1), BDNCA-325 ($\lambda_{abs}/\lambda_{em} = 558/585$ nm, extinction cooefficient $\varepsilon = 58,000 \, M^{-1} cm^{-1}$, quantum yield $\Phi = 0.06$) was chosen as the most selective for the beta TC-6 cells (Figure 1a) in comparison to the two control cell types in terms of relative fluorescence intensity. The BDNCA library was prepared from a BODIPY-aniline (BDN) series by chloroacetylation. While BDN has very low fluorescence emission (less than 1% quantum yield) owing to photoinduced electron transfer (PET), by converting the amine to an amide, the fluorescence of BDNCA was moderately increased ($\Phi = 5$–10%). Therefore, this amide motif is a modulator of the fluorescence intensity of the BDNCA series through interaction with the surrounding environment or binding partner.

However, when we injected BDNCA-325 intravenously into a mouse, the pancreatic islets were not selectively stained at various incubation times and concentrations (data not shown). Because BDNCA-325 contains a chemically reactive chloroacetyl group, we hypothesized that the compound might have reacted with other tissues in the animal before reaching the pancreatic islets. Thus, BDNCA-325 was modified by removing the reactive alpha-chloride and also by

[*] Dr. N.-Y. Kang, Dr. S.-C. Lee, Dr. S.-J. Park, Dr. S.-W. Yun, Dr. E. Kostromina, Dr. N. Gustavsson, Dr. Y. Ali, Y. Chandran, Dr. W. Han, Dr. G. K. Radda, Prof. Y.-T. Chang
Singapore Bioimaging Consortium, Agency for Science, Technology and Research (A*STAR)
138667, Singapore (Singapore)
E-mail: chmcyt@nus.edu.sg
Homepage: http://ytchang.science.nus.edu.sg

Prof. Y.-T. Chang
Department of Chemistry and MedChem Program of Life Sciences Institute, National University of Singapore
117543 Singapore (Singapore)

Prof. H.-H. Ha
Department of Pharmacy, Sunchon National University
Sunchon (Korea)

Dr. H. S. Chun, Dr. M. A. Bae, Dr. J. H. Ahn
Drug Discovery Division, Korea Research Institute of Chemical Technology
Yuseong-Gu, Daejeon, 305-600 (Korea)

Supporting information for this article is available on the WWW under http://dx.doi.org/10.1002/anie.201302149.
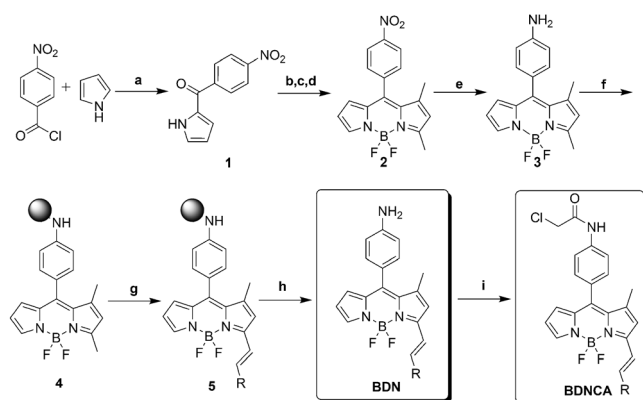
Scheme 1. a) MeMgBr, THF, −78 °C→25 °C, overnight; b) NaBH$_4$, 0 °C→25 °C, THF/MeOH (10:1), 2 h; c) 2,4-dimethyl pyrrole, InCl$_3$, CH$_2$Cl$_2$; d) 1) DDQ in CH$_2$Cl$_2$, 2) BF$_3$-Et$_2$O, TEA; e) Pd/C, hydrazine monohydrate, EtOH, reflux, 2 h; f) 2-chlorotrityl resin, pyridine; g) pyrrolidine, RCHO*, 300 W microwave, 2 minutes NMP/nBuOH (4:1); h) 0.5 % TFA in CH$_2$Cl$_2$; i) ClAcCl, NaHCO$_3$, acetonitrile/CH$_2$Cl$_2$ (1:1); THF = tetrahydrofuran, DDQ = 2,3-dichloro-5,6-dicyanobenzoquinone, TEA = triethylamine, NMP = N-methyl-2-pyrrolidone, TFA = trifluoroacetic acid, *RCHO is from commercially available number 237 of aldehyde building block (Supporting Information, Table S1).

changing the chain length of the acryl group. Among the various derivatives of BDNCA-325 tested, the acetyl derivative showed clear pancreatic islet staining upon tail-vein injection (Figure 1b), and thus was named pancreatic islet yellow (**PiY**; $\lambda_{abs}/\lambda_{em} = 558/585$ nm, $\varepsilon = 56,300\,\text{M}^{-1}\,\text{cm}^{-1}$, $\Phi = 0.05$). **PiY** also could be used in vivo for staining the islets of Langerhans, by showing the three-dimensional structures along with staining of the encircled blood vessel with FITC-dextran (Figure 1c). By incubating **PiY** for different times following a 50 µM injection, we found that one hour incuba-

tion was the optimal staining time with the lowest background signal and highest contrast (Supporting Information, Figure S1a). On the other hand, the current standard dye for pancreatic islet staining in vitro, Newport Green DCF diacetate did not show selective staining in a similar injection experiment (Supporting Information, Figure S1b). To confirm the beta cell selectivity of **PiY**, we sorted out **PiY** stained cells from the islets using FACS and analyzed the mRNA expression level of insulin, which is a marker for beta cells. The top 15 % of the **PiY**$^{\text{Bri}}$ and **PiY**$^{\text{Dim}}$ populations were isolated and analyzed for their relative mRNA levels by real-time PCR, which clearly showed that **PiY**$^{\text{Bri}}$ cells were highly enriched with beta cells compared to **PiY**$^{\text{Dim}}$ cells (Supporting Information, Figure S2). This is the first demonstration of a fluorescent small-molecule probe that can selectively stain pancreatic islets by injection into live animals.

Measurement of the mass of healthy beta cells is an important index for diagnosing diabetes. **PiY** staining clearly showed fewer islets (also with lower intensity) in the streptozotocin (STZ)-treated type 1 diabetic mouse model compared to healthy mouse islets (Figure 2c). There was a good correlation between **PiY** staining and insulin antibody immunostaining (Figure 2a,b). This **PiY** staining method is much simpler and faster than insulin-antibody-based immunostaining, which requires several steps of sample handling and thus is not practical for statistical analysis.

Finally, we applied **PiY** staining to harvest pancreatic islets from the total pancreas. The isolation of pancreatic islets usually requires a high level of technical experience and labor-intensive methods, partly because of the difficulty in visual identification of the islets. In situ staining of the islets by **PiY** made visual inspection of the islets extremely easy and the isolation of islets using the fluorescence surgical procedure was feasible, even for a minimally trained researcher (Supporting Information, Figure S3a). To confirm the safety
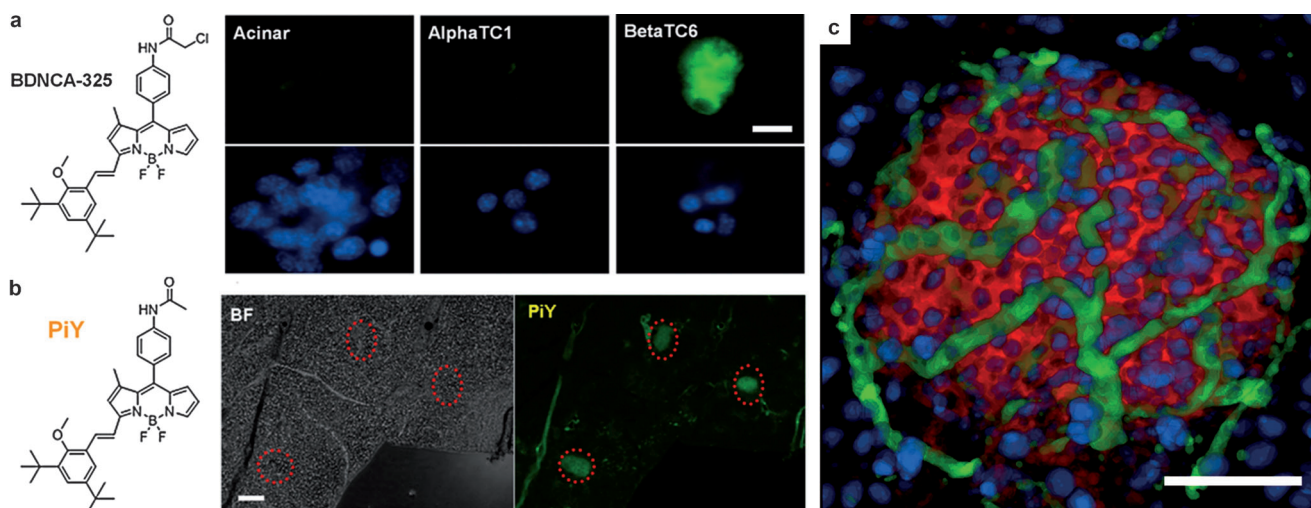

Figure 1. Visualizing pancreatic islets using **PiY** staining in vivo. a) Chemical formula of BDNCA-325 and the fluorescent cell culture images of staining by BDNCA-325 and Hoechst 33342 (nuclear stain). Upper panels: fluorescent images using a TRITC filter for BDNCA-325; lower panels: fluorescent images using a DAPI filter for Hoechst 33342. Scale bar = 10 µm. b) Chemical formula of **PiY** and pancreas tissue section images of **PiY** stained islets. 50 µM of **PiY** was administrated to the mouse tail vein for one hour. Scale bar = 200 µm. c) 3D structure processed image of a pancreatic islet. The fluorescent images of **PiY** (red) and FITC-dextran (green) were taken using TRITC and FITC channels, respectively. DAPI (blue) stain shows nuclei. Scale bar = 50 µm.
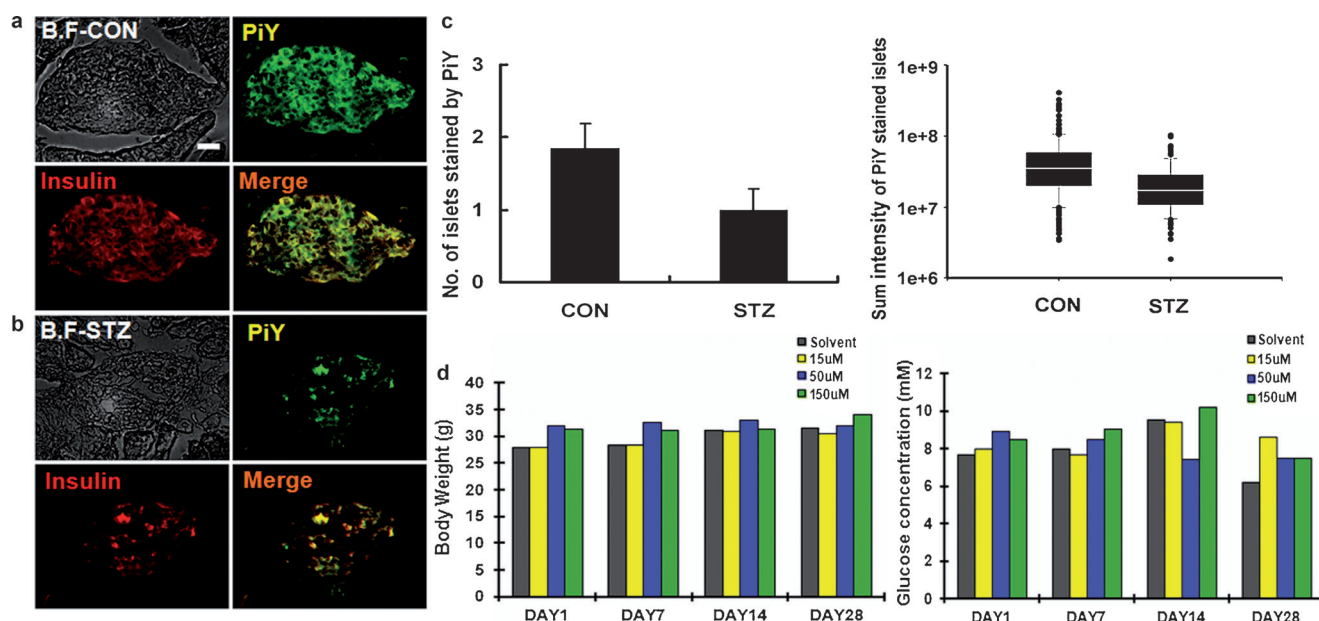
Figure 2. Selective staining of healthy islets and in vivo toxicity study of **PiY**. a) Fluorescence images of a **PiY** stained healthy islet using a TRITC filter. Subsequently, the same islet images were confirmed by immunostaining with an insulin antibody using a Cy5 filter. Scale bar = 20 μm. b) Fluorescence images of **PiY** stained STZ-induced mouse islet. 150 mg kg^{-1} of streptozotocin was injected as a single dose intraperitoneally and monitored for 9 days. Subsequently, **PiY** was injected for one hour. The same **PiY** stained islet images were confirmed by immunostaining with an insulin antibody. c) Total number of **PiY** stained islets and sum intensity of **PiY** stained islets. $n = 3$ for both CON and STZ mice with 300 sections per mouse ($p < 0.01$). d) Change of mouse body weight and blood glucose level during 28 days of **PiY** injection ($n = 1$). Blood was taken from the mouse tail and tested using a blood glucose meter (Lifescan Inc., USA).

of **PiY** as an imaging probe for functional islets, we further tested the effect of the probe on the islets. We tested for insulin release from the isolated islets and **PiY** did not affect the amount of insulin secreted upon glucose stimulation compared to the empty vehicle (Supporting Information, Figure S3 b). In addition, there was no detectable change by **PiY** on body weight or blood glucose levels of mice for at least a month following **PiY** injection at various concentrations, even at high doses up to 150 μM of the probe (Figure 2 d).

To examine the effect of the probe in different species, we further tested **PiY** in rats by tail-vein injection, and a selective staining of pancreatic islets was clearly demonstrated after one and four hours incubation (Supporting Information, Figure S4). With the promising data from the rats, we carried out a pharmacokinetic study on rats and all the parameters are summarized in the Supporting Information, Figure S5 a. When injected, almost all **PiY** existed as a bound form in human and rat blood plasma (99.4 ± 0.3 and 99.7 ± 0.1 %). The plasma concentration of **PiY** reached a maximum at five hours and slowly decreased with a half-life $t_{1/2}$ of 15 hours (Supporting Information, Figure S5 b). At 24 hours after injection of **PiY** in the rat tail vein, we collected pancreas, lung, liver, and brain tissues and measured the concentration of residual **PiY**. While the concentration in the brain was very low, lung and liver samples showed higher **PiY** signal than pancreas (Supporting Information, Figure S5 c). The trend was similar for a shorter time point (0.5 hours after tail vein injection), showing that the **PiY** concentration was higher in the liver, lungs, and heart than in the pancreas and even lower in the stomach, intestines, brain, and testes (Supporting

Information, Figure S6). This data showed that **PiY** is selective for islet staining among pancreatic cells as designed for the original screening (alpha, beta, and acinar cells), but not for other organ cells. For intact animal imaging, **PiY** could be used only when combined with another anatomical modality of imaging such as MRI or X-ray CT.

Finally, the elucidation of the cellular target protein of **PiY** would be extremely useful for understanding the molecular mechanism of the selective staining of beta cells by **PiY**. We tried most of the conventional target identification techniques including an affinity matrix and activity-based protein profiling, but could not convincingly identify the molecular target. Further studies with more sophisticated techniques are underway to understand the unique binding properties of **PiY**.

In conclusion, we developed the first fluorescent small molecule probe **PiY** for live-animal pancreatic islet staining. Through a simple tail-vein injection, **PiY** stains pancreatic islets without toxicity or functional disturbance of the beta cells, demonstrating its potential to quantitatively measure healthy islets and as a marker for facile islet surgical separation. In situ islet imaging using **PiY** will be important not only for the study of diabetes and the measurement of healthy islets, but also to further investigate beta cell development and islet transplantation.

Experimental Section

Injection of **PiY** for both in vivo staining and isolation of islets was carried out at 50 μM in the mouse tail vain for one hour. A stock

solution in DMSO of PiY (1 mM) was dissolved in PBS with 1% poly(ethylene glycol) (M.W. = 4600 Da) and 0.1% Tween 20 to make a 50 μM **PiY** injection solution. 250 μL of **PiY** injection solution was administrated.

In vivo staining of **PiY**: After **PiY** injection, the dissected pancreas was fixed using 4% paraformaldehyde (PFA) for three hours at 4°C and changed with fresh PBS for one hour at 4°C. Subsequently, the fixed pancreas was incubated overnight in 30% sucrose at 4°C. The following day, the pancreas was embedded in an optimal cutting temperature compound for one hour at −80°C and followed by incubation in the cryo machine (set below −20°C) for one hour. The cryo-pancreas block was sectioned into 10 μm thick slices. The sections on slides were air-dried at room temperature for 30 min and stored at 4°C until use. To observe **PiY**-stained islets, the pancreatic sections were washed with PBS for 5 minutes and the sections were observed using fluorescent microscopy on the TRITC channel for **PiY**.

Isolation of **PiY**-stained islets: Extracted pancreas was immediately transferred into a vial containing cold Krebs–Ringer–Hepes (KRH) medium (130 mM NaCl, 4.7 mM KCl, 1.2 mM KH_2PO_4, 1.2 mM MgSO4, 2.56 mM $CaCl_2$, 1 mgmL^{-1} BSA, 20 mM Hepes, pH 7.4) and cut into smaller pieces. Collagenase-P (0.5 mgmL^{-1}; Roche) was added and the vial was placed into a 37°C water bath shaker (180–200 rpm) for 15–20 minutes. After digestion, cold KRH buffer with 0.1% BSA was added and the vial was inverted several times. The suspension was washed away after allowing the islets to settle to the bottom of the vial for 10 minutes and this wash process was repeated twice more. After picking islets from **PiY** and control solutions, they were transferred to a new glass-bottom dish to observe using fluorescent microscopy.

[1] C. M. Benitez, W. R. Goodyer, S. K. Kim, *Cold Spring Harbor Perspect. Biol.* **2012**, *4*, a012401.

[2] N. V. Evgenov, Z. Medarova, J. Pratt, P. Pantazopoulos, S. Leyting, S. Bonner-Weir, A. Moore, *Diabetes* **2006**, *55*, 2419–2428.

[3] A. Hörnblad, U. Ahlgren, *Islets* **2009**, *1*, 163–164.

[4] U. Ahlgren, M. Gotthardt, *Adv. Exp. Med. Biol.* **2010**, *654*, 39–57.

[5] Y. B. Ahn, G. Xu, L. Marselli, E. Toschi, S. Sharma, S. Bonner-Weir, D. C. Sgroi, G. C. Weir, *Diabetologia* **2007**, *50*, 334–342.

[6] B. Lukowiak, B. Vandewalle, R. Riachy, J. Kerr-Conte, V. Gmyr, S. Belaich, J. Lefebvre, F. Pattou, *J. Histochem. Cytochem.* **2001**, *49*, 519–528.

[7] J. I. Conget, Y. Sarri, J. M. Gonzalez-Clemente, R. Casamitjana, M. Vives, R. Gomis, *Pancreas* **1994**, *9*, 157–160.

[8] S. Speier, D. Nyqvist, O. Cabrera, J. Yu, R. D. Molano, A. Pileggi, T. Moede, M. Kohler, J. Wilbertz, B. Leibiger, C. Ricordi, I. B. Leibiger, A. Caicedo, P. O. Berggren, *Nat. Med.* **2008**, *14*, 574–578.

[9] T. Reiner, G. Thurber, J. Gaglia, C. Vinegoni, C. W. Liew, R. Upadhyay, R. H. Kohler, L. Li, R. N. Kulkarni, C. Benoist, D. Mathis, R. Weissleder, *Proc. Natl. Acad. Sci. USA* **2011**, *108*, 12815–12820.

[10] C. N. Im, N. Y. Kang, H. H. Ha, X. Bi, J. J. Lee, S. J. Park, S. Y. Lee, M. Vendrell, Y. K. Kim, J. S. Lee, J. Li, Y. H. Ahn, B. Feng, H. H. Ng, S. W. Yun, Y. T. Chang, *Angew. Chem.* **2010**, *122*, 7659–7662; *Angew. Chem. Int. Ed.* **2010**, *49*, 7497–7500.

[11] Y. K. Kim, J. S. Lee, X. Bi, H. H. Ha, S. H. Ng, Y. H. Ahn, J. J. Lee, B. K. Wagner, P. A. Clemons, Y. T. Chang, *Angew. Chem.* **2011**, *123*, 2813–2815; *Angew. Chem. Int. Ed.* **2011**, *50*, 2761–2763.

[12] S. W. Yun, C. Leong, D. Zhai, Y. L. Tan, L. Lim, X. Bi, J. J. Lee, H. J. Kim, N. Y. Kang, S. H. Ng, L. W. Stanton, Y. T. Chang, *Proc. Natl. Acad. Sci. USA* **2012**, *109*, 10214–10217.

[13] N. Y. Kang, H. H. Ha, S. W. Yun, Y. H. Yu, Y. T. Chang, *Chem. Soc. Rev.* **2011**, *40*, 3613–3626.

[14] J. S. Lee, N. Y. Kang, Y. K. Kim, A. Samanta, S. Feng, H. K. Kim, M. Vendrell, J. H. Park, Y. T. Chang, *J. Am. Chem. Soc.* **2009**, *131*, 10077–10082.

[15] M. Brissova, M. Shiota, W. E. Nicholson, M. Gannon, S. M. Knobel, D. W. Piston, C. V. Wright, A. C. Powers, *J. Biol. Chem.* **2002**, *277*, 11225–11232.

[16] M. Vendrell, G. G. Krishna, K. K. Ghosh, D. Zhai, J. S. Lee, Q. Zhu, Y. H. Yau, S. G. Shochat, H. Kim, J. Chung, Y. T. Chang, *Chem. Commun.* **2011**, *47*, 8424–8426.